Supporting Information

Straight-chain Thiols as Chemical Kinetic Transporters Accelerate Li_2S 3D Nucleation

Wenchang Han[a], Jiyue Hou[a], Bao Zhang[a], Yongqi Wang[a], Chunman Yang[a], Wengxiang Ai[a], Qian Wang[a], Enfeng Zhang[a], Peng Dong[a], Yiyong Zhang[a,] *, Yingjie Zhang[a,] *, Yannan Zhang[a,] *

[a] National local joint engineering research center for Lithium-ion Batteries and Materials Preparation Technology, Key Laboratory of Advanced Batteries Materials of Yunnan Province, Faculty of Metallurgical and Energy Engineering, Kunming University of Science and Technology, Kunming 650093, China

Experimental section

Preparation of electrolyte

The materials and solvents used in this study were obtained from commercial sources such as Aldrich, RHAWN, and Dodochem. The baseline electrolyte consisted of a mixture of two lithium salts: 1 M lithium bis (trifluoromethane sulfonyl) imide (LiTFSI) and 2.0 wt.% $LiNO_3$, and two solvents, 1,2-diamethyl ethane (DME)/1,3-dioxolane (DOL) (v/v = 1:1). 1,8-Octanedithiol (1,8-OT), 1-octanedithiol (1-OT), 1,6-hexanedithiol (1,6-HT), 1,10-decanedithiol (1,10-DT) were added to the blank electrolyte at different weight ratios (0.5 wt.%, 1 wt.%, 2 wt.%, 3 wt.%, 5 wt.%) and then stirred to form a homogeneous solution. All preparation processes of this work were performed in an argon-filled glove box with oxygen and moisture content controlled below 0.01 ppm.

Preparation of sulfur cathode

Sulfur carbon composite materials are obtained by sintering conductive carbon (Super P) and sublimated sulfur in a weight ratio of 3:7. Grind the mixture in a mortar and pestle for 30 minutes to ensure uniform mixing. Place the resulting mixture in a crucible and keep it at 155 ° C for 12 hours in a tube furnace filled with argon gas. Mix and grind the sulfur carbon composite material, Super P, and adhesive PVDF in a weight ratio of 7:2:1, prepare a pulp with N-methyl-2-pyrrolidone (NMP) and coat it on an aluminum foil collector, and dry it in a vacuum oven at 60 ° C for 8 hours. Finally, cut the dried electrode into discs with a diameter of 12 mm. The sulfur content of the positive electrode is 49%. The sulfur loading in this article is approximately 1.2 mg cm^{-2}. By adding blank electrolytes or electrolytes containing linear thiols, the electrolyte sulfur ratio (E/S) is fixed at 30 μL mg^{-1}. Carbon paper was used as the collector for high sulfur loading, and the sulfur-carbon composite and PVDF were pulped and coated on the carbon paper at 9:1, and finally the

polar sheet with a surface loading of 4.1 mg cm^{-2} was obtained, with a controlled E/S ratio of 10 μL mg^{-1}. lithium-sulfur coin batteries are assembled using a stainless-steel battery box (2025 model) in an argon filled glove box.

Preparation of polysulfides

Sublimated sulfur (Aladdin, 99.5%) and lithium sulfide (Aladdin, 99.9%) were added to the baseline electrolyte in molar ratios of 5:8 and 7:8, respectively. The mixture was magnetically stirred at 60 °C for 72 hours to form a dark brown solution (Li_2S_6 and Li_2S_8). All operations were performed in an argon-filled glove box.

Electrochemical measurements

The cycling and multiplication performance of the lithium-sulfur batteries (LSBs) were tested on a Land Test System with a voltage range of 1.7-2.8 V. CV measurements were performed using the LANHE Test System. The CV measurements were made at a sweep rate of 0.1 mV s^{-1} over the voltage range of 1.7-2.8 V, and the variable-speed CVs were swept at rates of 0.1, 0.2, 0.3, 0.4, and 0.5 mV s^{-1}. Electrochemical impedance spectroscopy (EIS) measurements and ionic conductivity measurements were performed using an Autolab electrochemical workstation with a frequency range of 100 kHz to 0.01 Hz and an AC excitation signal of 10 mV. LBSs was used for the EIS tests. The constant current intermittent titration (GITT) test was performed on a Neware Test System with a pulsed constant current of 0.2 mA, a relaxation time of 120 s, and a voltage range of 1.7-2.8 V.

The diffusion coefficient of Li^+ during sulfur redox can be measured according to the classical Randles-Sevcik equation:

$$I_P = 2.69 \times 10^{-5} \times n^{3/2} \times A \times D_{Li^+}^{1/2} \times v^{1/2} \times C_{Li^+} \quad (1)$$

where I_P is the peak current, n (n =2) is the number of electrons in the reaction, A (A = 1.13 cm^{-2}) is the electrode area, D_{Li^+} is the Li^+ diffusion coefficient, ν is the scan rate, and

C_{Li^+} ($C_{Li^+} = 1\times10^{-3}$ mol mL^{-1}) is the Li^+ concentration in the electrolyte. There is a positive correlation between the slope of the curve and the corresponding Li^+ diffusion. Based on the linear relationship between $v^{1/2}$ and I_P, the Li^+ diffusion coefficient of the obtained material can be calculated.

To investigate the effect of 1-OT/1,8-OT on polysulfide conversion and Li_2S deposition, Li|Li_2S_8 and Li|Li_2S_8 + 1-OT/1,8-OT cells (CR2016) were assembled. The anode consisted of lithium foil, the cathode utilized carbon paper, and a Celgard 2500 diaphragm was employed. The Li|Li_2S_8 cell was filled with 30 μL of 0.1 M Li_2S_8 solution and 15 μL of blank electrolyte, while the Li|Li_2S_8+1-OT/1,8-OT cell contained 30 μL of 0.1 M Li_2S_8 solution and 15 μL of electrolyte with 2 wt% 1-OT/1,8-OT. The cells were discharged at a constant current of 0.112 mA to 2.11 V, and then discharged at a constant potential of 2.09 V to promote nucleation and growth of Li_2S until the current dropped below 10^{-5}A. All the above tests were performed multiple times to ensure accuracy and reproducibility of the data, while stability was continuously monitored during the tests. The capacity contribution of thiols was verified by using carbon paper as cathode and a mixture of 1,8-OT+S_8 as active material.

Characterization

The reaction products of 1-OT/1,8-OT with Li_2S_6 and S_8 were detected by gas chromatography-mass spectrometry (Agilent 8890-5977B), and the chemical formula of the reaction products was inferred based on the mass to charge ration (m/z). Li_2S_6 and its reacted substances were characterized using a Thermo Fisher Scientific UV vis spectrometer and a Raman spectrometer (model LabRAM HR). Photographs were taken for visualization purposes during the experiments. Furthermore, in-situ Raman testing was conducted on lithium-sulfur batteries during charge and discharge cycles using a LabRAM HR Raman spectrometer. Microscopic images of the positive electrode during discharge

were also captured. To confirm the reduction of side reactions of polysulfides and lithium anodes by the addition of 1-OT/1,8-OT, the LSBs were disassembled after 10 cycles. The internal lithium foils were collected, cleaned with dimethoxymethane (DME), and dried in an argon-filled glove box. The surface morphology of the lithium anode was observed using scanning electron microscopy (SEM). After the constant potential test, the carbon paper was cleaned with DME and the deposition of Li_2S was observed by SEM. Additionally, X-ray photoelectron spectroscopy (XPS) was utilized to analyze the chemical composition of the cathode surfaces after cycling.

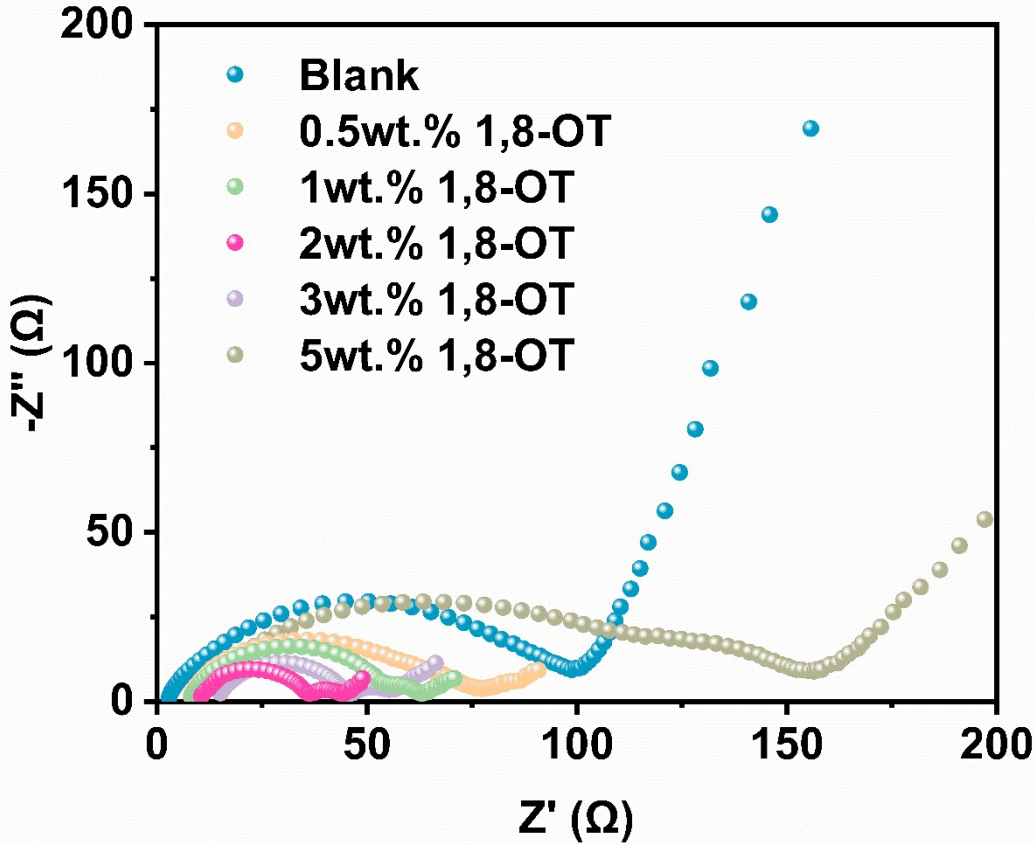

Fig. S1. Electrochemical impedance spectra of LSBs with different 1,8-OT contents

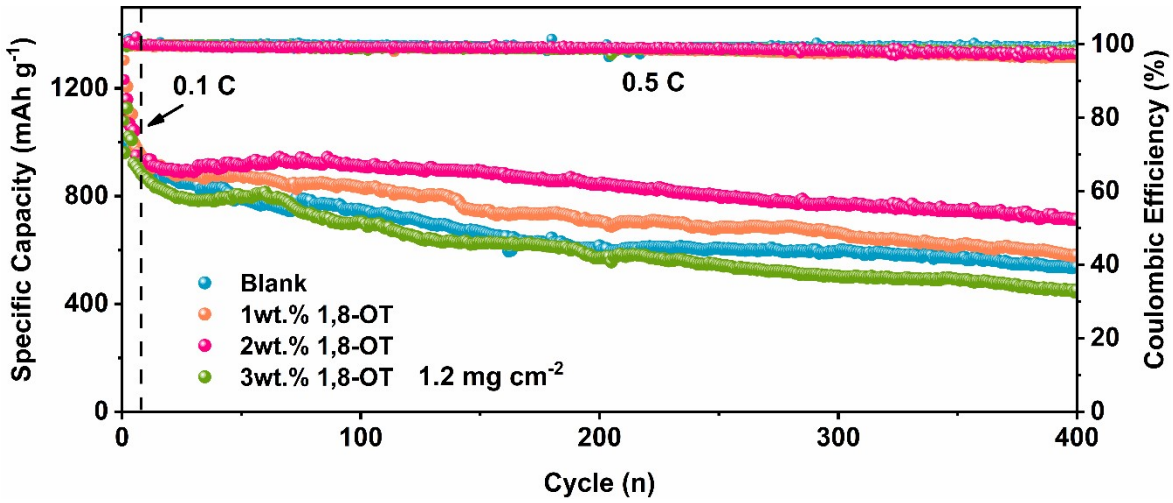

Fig. S2. Cycle performance curves of lithium sulfur batteries with different 1,8-OT contents at 0.5 C.

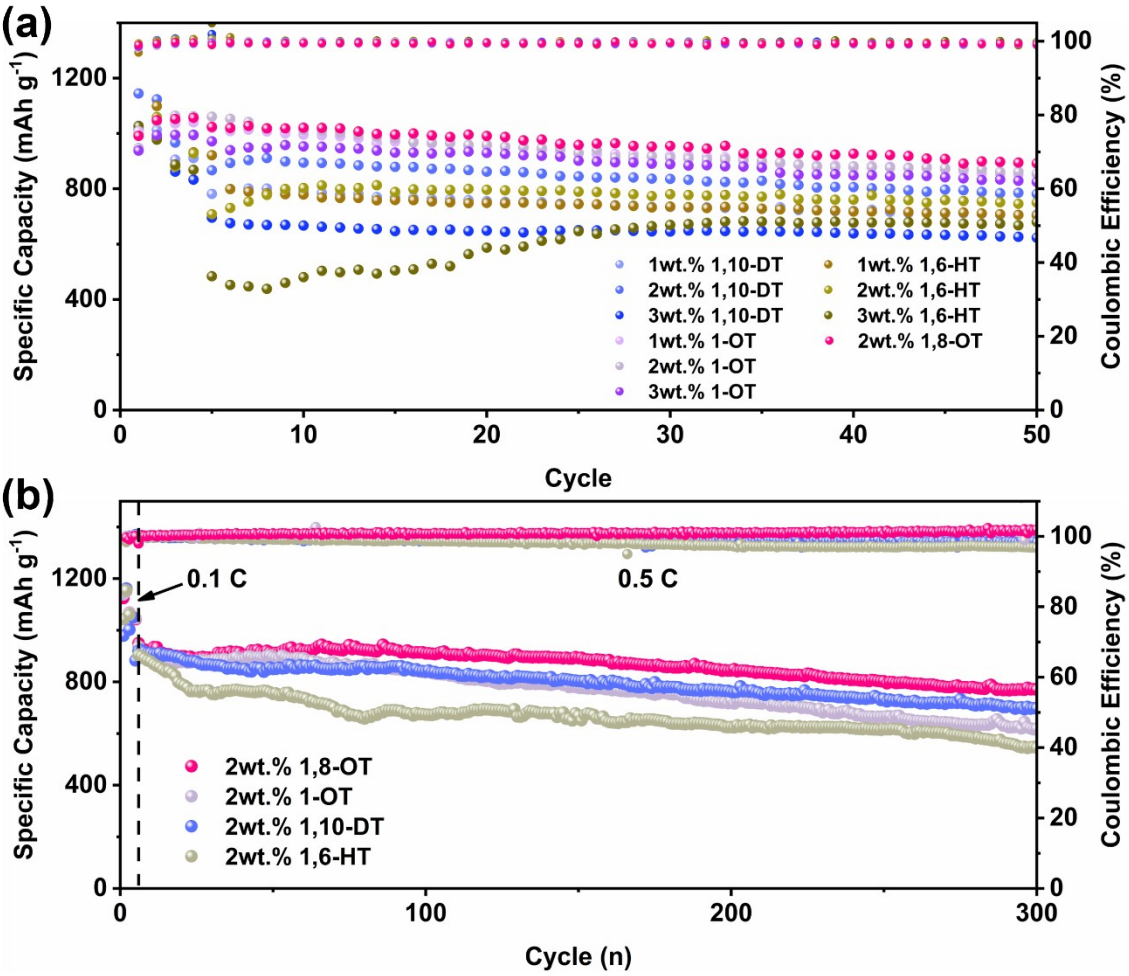

Fig. S3. (a) Cycling performance of different concentrations and types of straight-chain thiols at 0.5 C, (b) Cycling performance curves of lithium-sulfur batteries containing different thiols at a concentration of 2wt.% at 0.5 C.

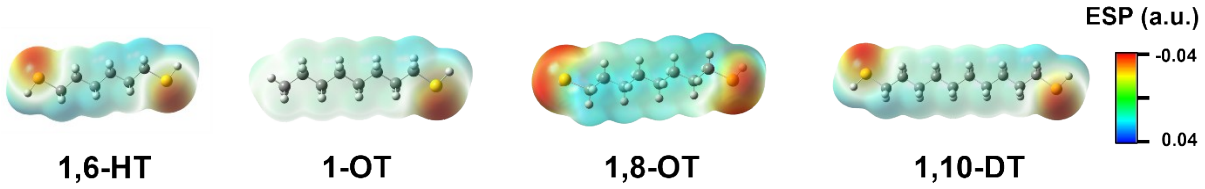

Fig. S4. Electrostatic potential (ESP) of 1,6HT, 1-OT, 1,8-OT, 1,10-DT.

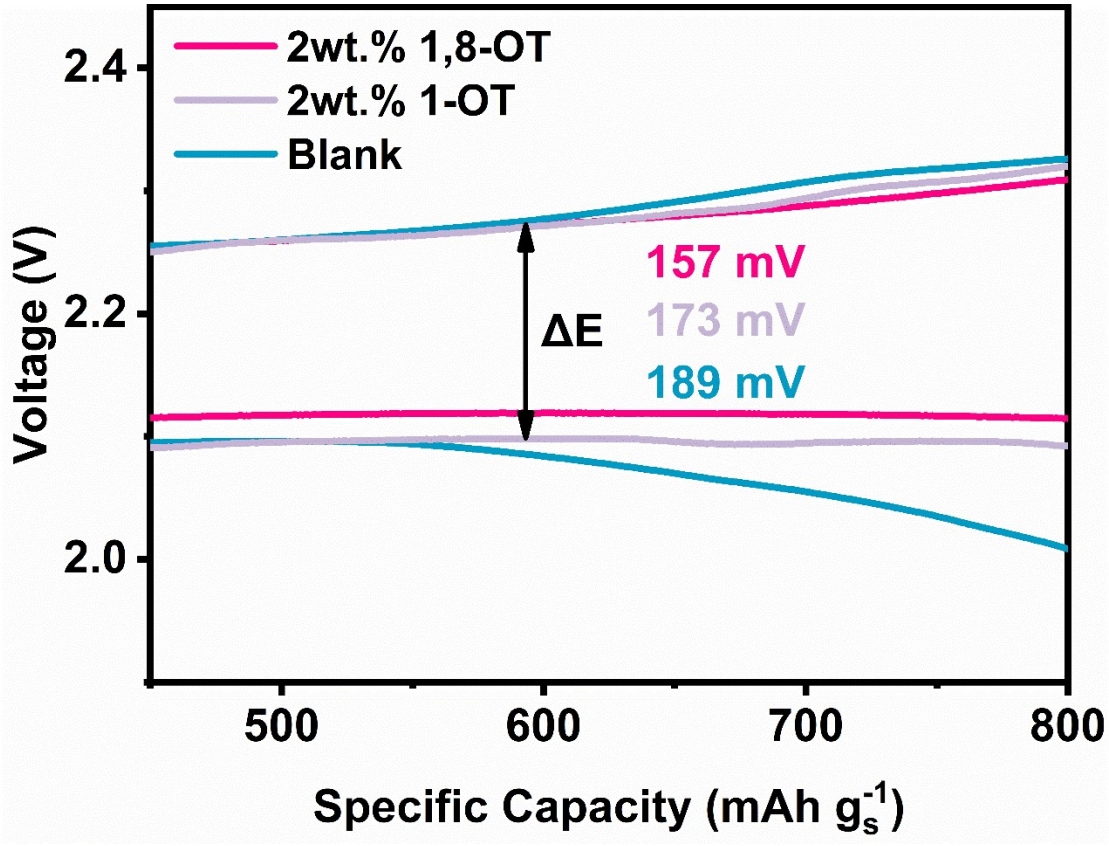

Fig. S5. Overpotential comparison in the plateau area of the replay curve at 0.2 C.

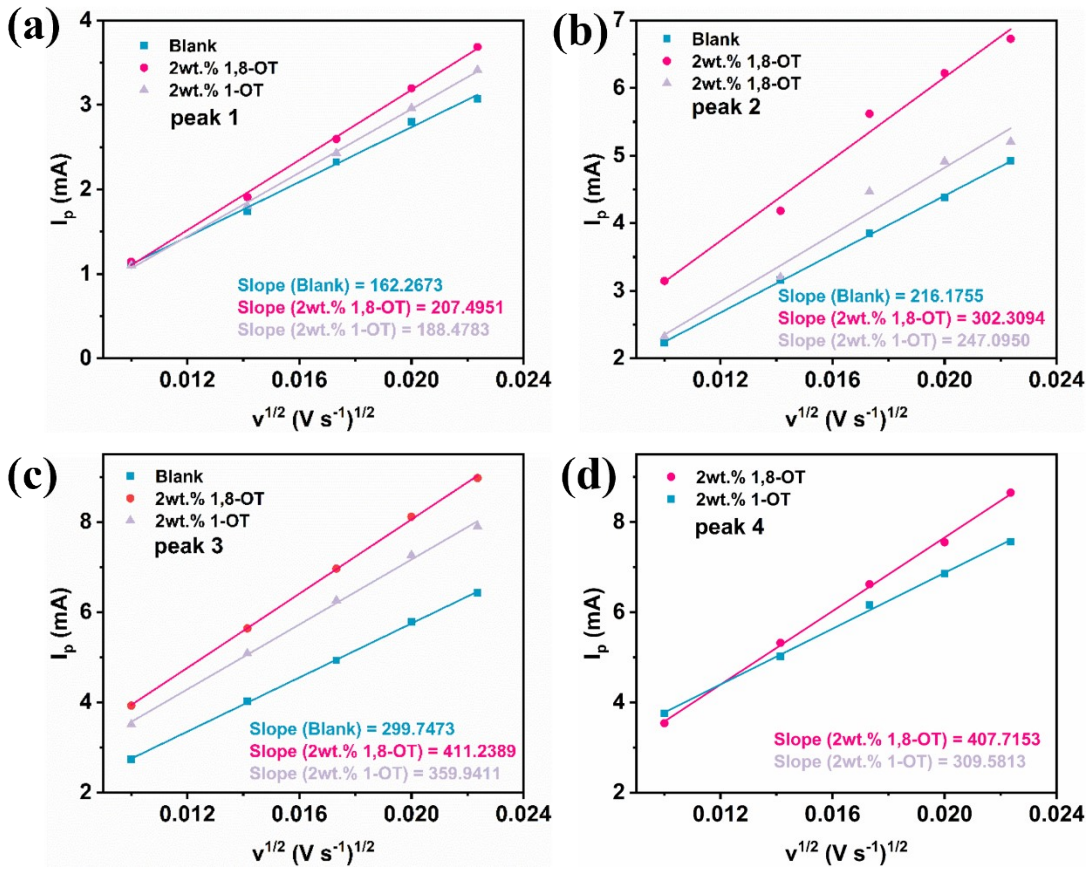

Fig. S6. Comparison of I_p - $v^{1/2}$ curves of different electrolytes, peak 1 (a), peak 1 (a), peak 2 (b), peak 3 (c), peak 4 (d).

Table S1. Lithium-ion diffusion coefficient data calculated based on the R-S equation and I_P-$v^{1/2}$ curves.

D_{Li}	Blank	2wt.% 1-OT	2wt.% 1,8-OT
Peak 1	**$3.56E^{-8}$**	**$4.80E^{-8}$**	**$5.81E^{-8}$**
Peak 2	**$6.31E^{-8}$**	**$8.25E^{-8}$**	**$1.23E^{-7}$**
Peak 3	**$1.21E^{-7}$**	**$1.75E^{-7}$**	**$2.28E^{-7}$**
Peak 4		**$1.29E^{-7}$**	**$2.25E^{-7}$**

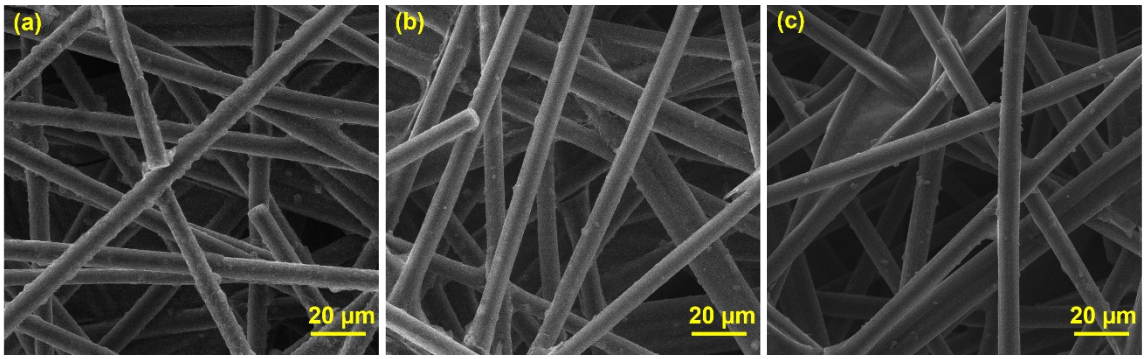

Fig. S7. Li_2S nucleation on carbon paper under SEM, (a) blank, (b) with 1-OT, (c) with 1,8-OT.

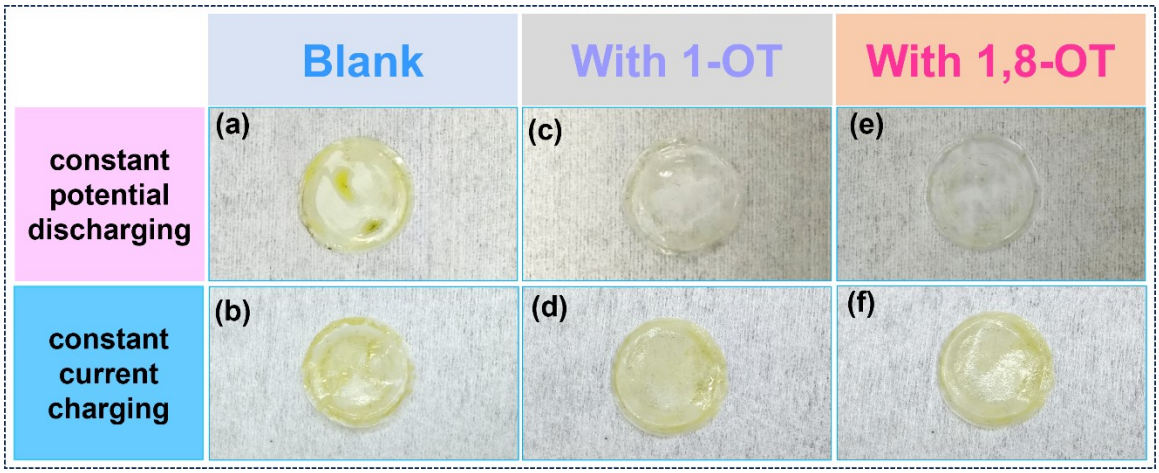

Fig. S8. Comparison of colours of disassembled battery separator after constant potential discharging and constant current charging, blank electrolyte (a, b), with 1-OT (c, d), with 1,8-OT (e, f).

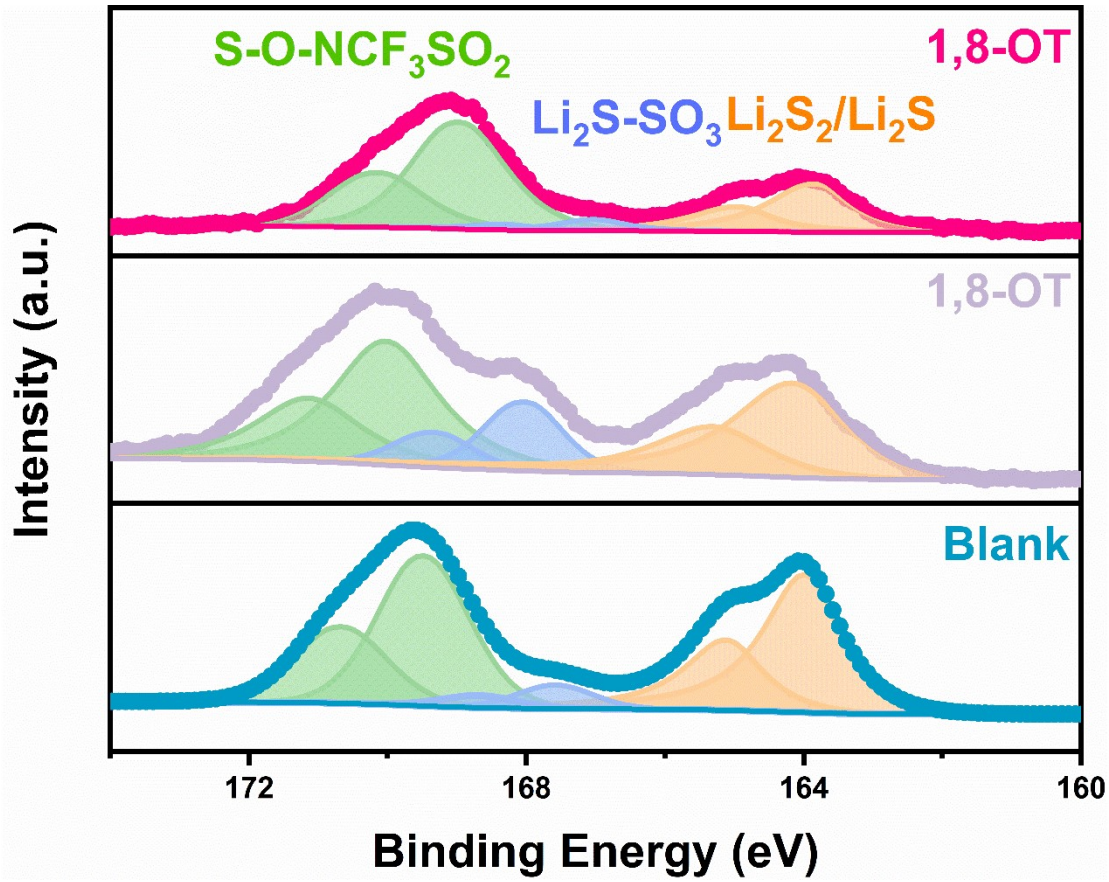

Fig. S9. S 2p XPS spectra of the cathode surface of lithium sulfur batteries containing different electrolytes after 5 cycles at 0.2 C.

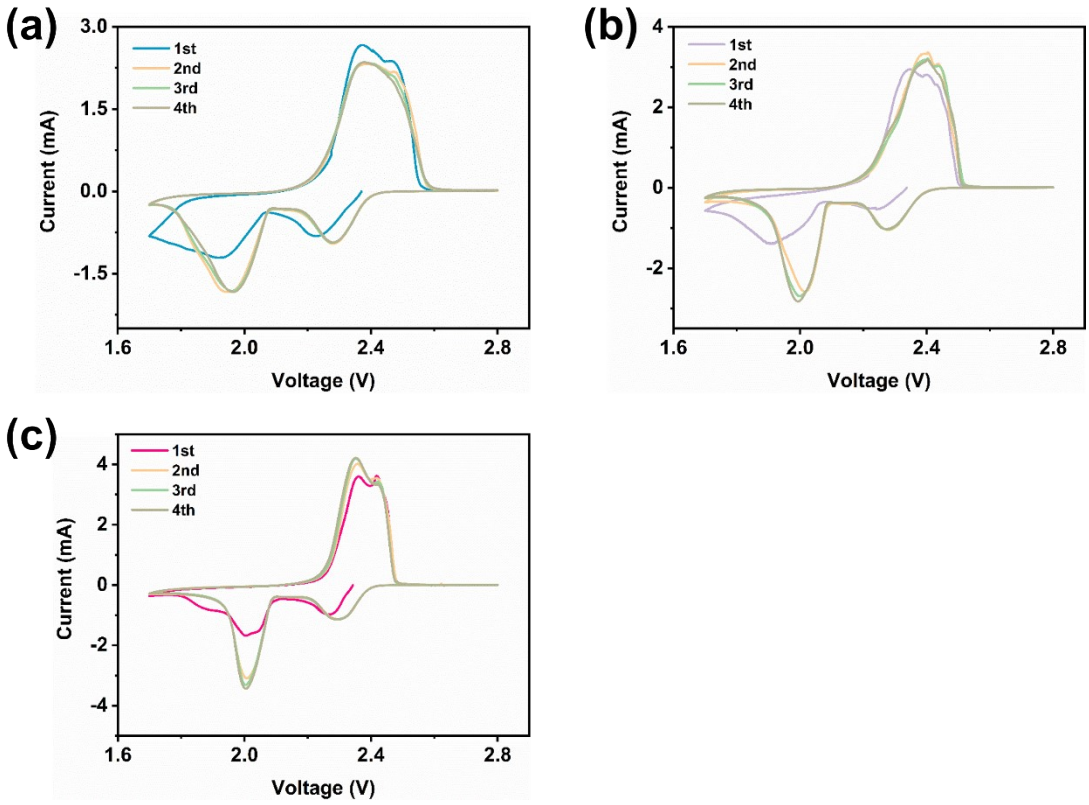

Fig. S10. CV curves of different cycles of lithium sulfur batteries containing different electrolytes, blank electrolyte (a), with 1-OT (b), with 1,8-OT (c).

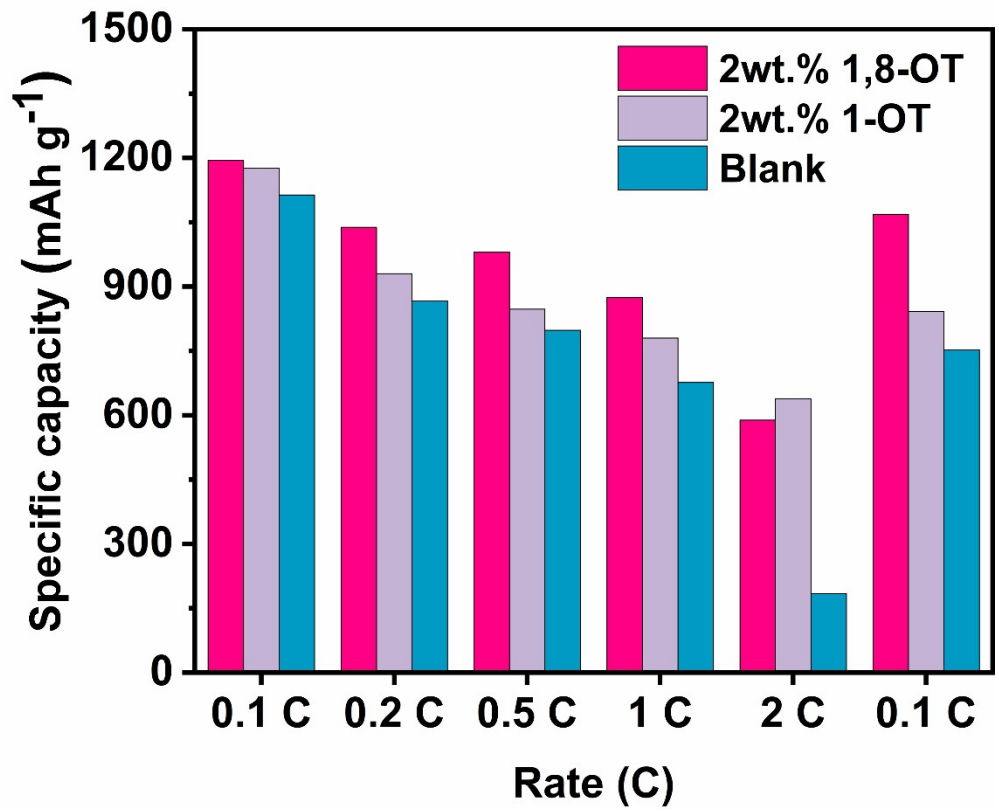

Fig. S11. Comparison of first lap capacity at different magnifications.

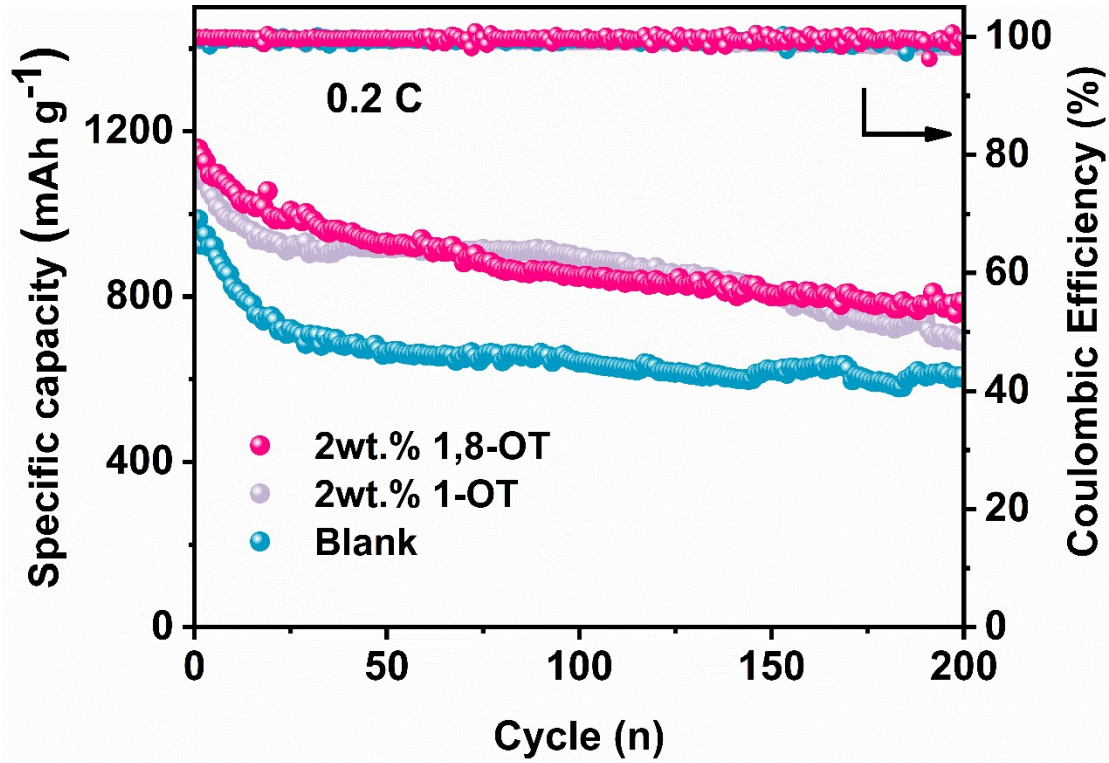

Fig. S12. Cycling performance at 0.2 C.

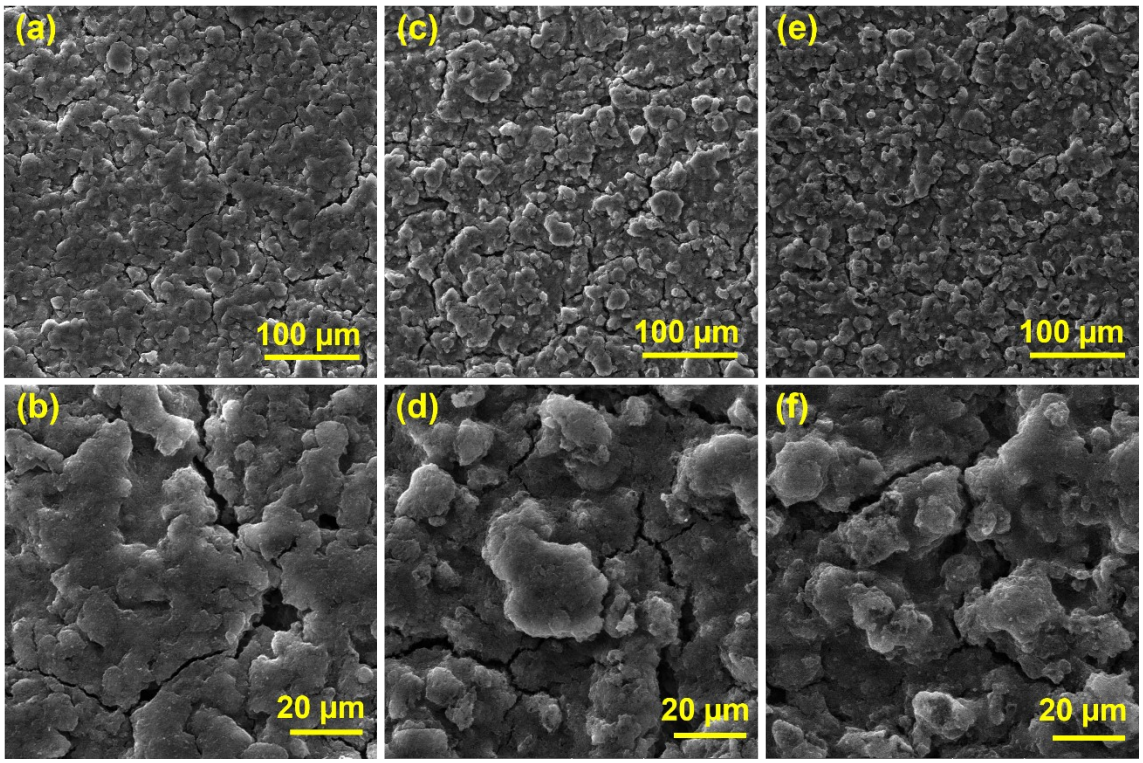

Fig. S13. Surface morphology of sulfur cathode after 400 cycles at 0.5C, blank electrolyte (a, b), with 1-OT (c, d), with 1,8-OT (e, f).

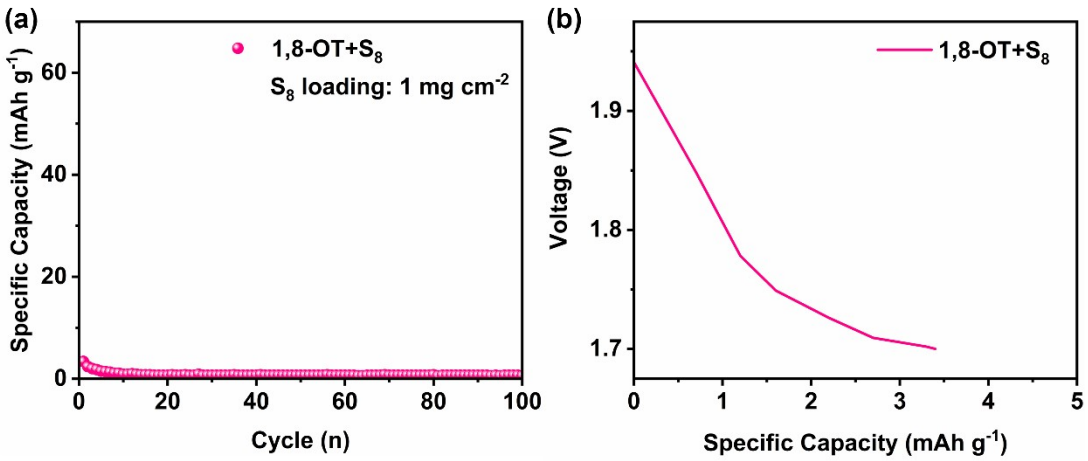

Fig. S14. Cycling performance at 0.1 C (a) and initial discharge curves (b) of batteries with carbon paper as cathode and a mixture of 1,8-OT+S_8 as active material.

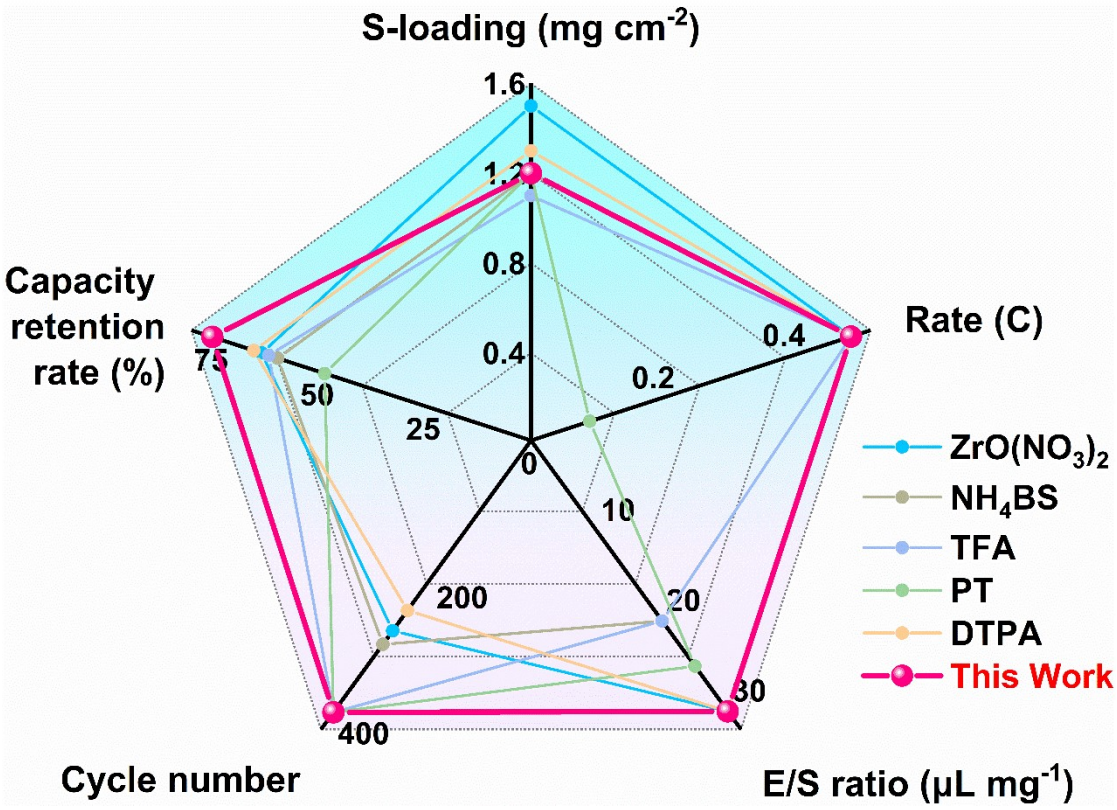

Fig. 15. Comparison of battery performance between this work and other studies ($ZrO(NO_3)_2$,[1] NH_4BS,[2] TFA,[3] PT,[4] DTPA[5]).

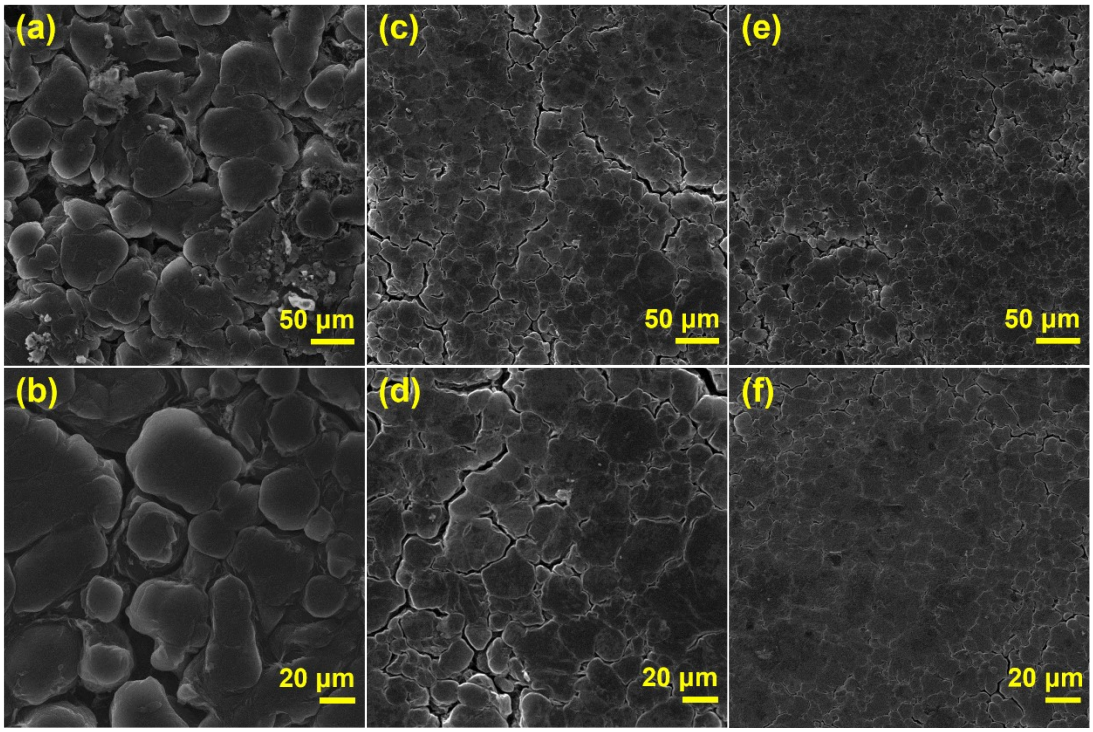

Fig. S16. The surface morphology of the lithium anode after cycling obtained by SEM, blank electrolyte (a, b), with 1-OT (c, d), with 1,8-OT (e, f).

Reference.

1. J. Li, L. Zhang, F. Qin, B. Hong, Q. Xiang, K. Zhang, J. Fang and Y. Lai, *J. Power Sources*, 2019, **442**, 227232.
2. J. Gu, D. Yang, X. Wang, Y. Song, Z. Li, H. Qiu, M. Wang, Q. Wang, B. Hong, Z. Zhang, J. Li and Y. Lai, *J. Colloid Interface Sci.*, 2023, **629**, 368-376.
3. L. He, S. Shao, C. Zong, B. Hong, M. Wang and Y. Lai, *ACS Appl. Mater. Interfaces*, 2022, **14**, 31814-31823.
4. Y.-Q. Peng, M. Zhao, Z.-X. Chen, Q. Cheng, Y. Liu, X.-Y. Li, Y.-W. Song, B.-Q. Li and J.-Q. Huang, *Nano Research*, 2023, **16**, 8253-8259.
5. S.-y. Shao, L. He, J.-w. Zhang, S.-m. Li, B. Hong, K. Zhang and J. Li, *J. Cent. South Univ.*, 2024, **31**, 431-442.